TRENDS IN COMPUTATIONAL STRUCTURAL MECHANICS
W.A. Wall, K.-U. Bletzinger and K. Schweizerhof (Eds.)

ON THE LACK OF SYMMETRY IN MATERIALS

Kaspar J. Willam[⋆]
University of Colorado Boulder
Boulder, CO 80309-0428, USA
e-mail: willam@colorado.edu
web page: http://www.civil.colorado.edu/~willam/

Maria-Magdalena Iordache
71 Fulkerson St., # 206
Cambridge, MA 02141, USA
Email: iordache@mit.edu

Abstract. In this paper we examine the loss of symmetry in mechanics of material. To this end we first review the so-called Bromwich bounds of eigenvalues in linear algebra. For illustration we revisit the hierarchy of different failure diagnostics when the material properties loose symmetry. Subsequently, we examine the lack of symmetry in the stress and strain measures which appears in finite deformation analysis and in micropolar continua. For definiteness, we evaluate maximum and minimum values of the non-symmetric second order tensors, which no longer coincide with the principal eigenvalues, and we discuss the special format of the trace invariants. For geometric visualization we generalize Mohr's circle and the underlying transformation relations which account for the loss of symmetry in two dimensions. To conclude, we consider two examples of shear failure which serve as model problems to address the intricate differences of symmetric and non-symmetric stress and deformation measures.

Key words: non-symmetric operators, material level, stress and strain level; principal eigenvalues, maximum and minimum values of normal and shear stresses, stress invariants, Mohr circle of non-symmetric second order tensors.

1 INTRODUCTION

Traditionally, we assume that the world of structures and materials is highly symmetric, i.e. the stiffness and compliance properties of structures are symmetric, and the underlying stress-strain relations are normally symmetric. Symmetry in the large is lost only at rare occasions, when non-conservative force systems are considered, or when convective transport terms are considered e.g. in fluid - structures interaction problems. Symmetry in the small is lost, when the material properties loose normality, e.g. due to non-associated plastic flow, or when they violate Onsager's principle of reciprocity in the absence of potentials. Even in these rare cases of non-symmetric material laws we resort to symmetric stress and strain measures to formulate the underlying constitutive relations. There are however a number of instances when the underlying measures of stress and strain themselves loose symmetry, such as in

(a) polar media, when couple stresses and micro-rotations enter the description of motion within the format of Cosserat continua, and in

(b) finite deformation problems, when the deformation gradient or the velocity gradient are used to describe finite deformations, and when the first Piola-Kirchhoff stress or the Mandel stress are used in the balance equations or as stress measure in the intermediate configuration.

The fundamental properties of symmetric versus non-symmetric operators may be best explained in terms of the Bromwich Bounds [1906] of linear algebra [**?**]. Though it applies to any complex matrix we consider here a real non-symmetric matrix which may be decomposed into symmetric and skew-symmetric components,

$$\mathbf{A} = \mathbf{A}^{sym} + \mathbf{A}^{skew} = \frac{1}{2}[\mathbf{A} + \mathbf{A}^t] + \frac{1}{2i}[\mathbf{A} - \mathbf{A}^t] \tag{1}$$

Consequently, the characteristic roots of $\mathbf{A}$ are in the complex plane, whereby the lowest and the highest eigenvalues of the symmetric and the skew-symmetric components bound the real and imaginary eigenvalues of the non-symmetric matrix. In short, the following eigenvalue bounds must hold,

Bromwich Bounds:

$$\lambda_{min}(\mathbf{A}^{sym}) \leq \Re(\lambda_i(\mathbf{A})) \leq \lambda_{max}(\mathbf{A}^{sym}) \tag{2}$$

and

$$\lambda_{min}(\mathbf{A}^{skew}) \leq \Im(\lambda_i(\mathbf{A})) \leq \lambda_{max}(\mathbf{A}^{skew}) \tag{3}$$

whereby the non-vanishing eigenvalues of the skewed symmetric matrix occur in conjugate pairs, i.e. $\sum_i \lambda_i(\mathbf{A}^{skew}) = 0$. Considering $\mathcal{D} \to \mathbb{R}^3$, one-out of the three eigenvalues is therefore always real-valued, while the other two might either be complex conjugate or real-valued in the case of real non-symmetric second order tensors.

2 HIERARCHY OF FAILURE INDICATORS

The Bromwich bounds help to explain the fundamental features of failure diagnostics which have occupied the mechanics community for a long period of time, when non-symmetric material properties were considered, $\dot{\boldsymbol{\sigma}} = \boldsymbol{\mathcal{E}}_{tan} : \dot{\boldsymbol{\epsilon}}$ with $\boldsymbol{\mathcal{E}}_{tan} \neq \boldsymbol{\mathcal{E}}^t_{tan}$. In this case, the singularities of different failure indicators [**?**] become active at different stages of the response history (see figure 1 for a schematic stress-strain diagram).

2.1 Loss of Material Stability

The traditional scalar product format of second order work density infers that only the symmetric components of the tangential material law are mobilized by the quadratic form,

$$d^2W = \dot{\boldsymbol{\sigma}} : \dot{\boldsymbol{\epsilon}} = \dot{\boldsymbol{\epsilon}} : \boldsymbol{\mathcal{E}}_{tan} : \dot{\boldsymbol{\epsilon}} = \frac{1}{2}\dot{\boldsymbol{\epsilon}} : [\boldsymbol{\mathcal{E}}_{tan} + \boldsymbol{\mathcal{E}}^t_{tan}] : \dot{\boldsymbol{\epsilon}} \tag{4}$$

When all possible deformation rates are considered, a zero value of the second order work density,

$$d^2W = 0 \quad \forall \dot{\boldsymbol{\epsilon}} \neq \mathbf{0} \tag{5}$$

is thus equivalent to a singularity of the symmetrized tangent stiffness,

$$\det(\frac{1}{2}[\boldsymbol{\mathcal{E}}_{tan} + \boldsymbol{\mathcal{E}}_{tan}^t]) = 0 \rightarrow \lambda_{min}(\frac{1}{2}[\boldsymbol{\mathcal{E}}_{tan} + \boldsymbol{\mathcal{E}}_{tan}^t]) = 0 \tag{6}$$

According to the Bromwich Bounds, the stability limiter bounds the spectral properties of $\lambda_n(\boldsymbol{\mathcal{E}}_{tan})$ from below when all possible strain rates are considered. In short, loss of material stability in the form $d^2W = 0$ precedes loss of uniqueness $\lambda_{min}(\boldsymbol{\mathcal{E}}_{tan}) = 0$ if non-symmetric material operators are considered, as

$$\lambda_{min}(\frac{1}{2}[\boldsymbol{\mathcal{E}}_{tan} + \boldsymbol{\mathcal{E}}_{tan}^t]) \leq \Re(\lambda_{min}(\boldsymbol{\mathcal{E}}_{tan})) \tag{7}$$

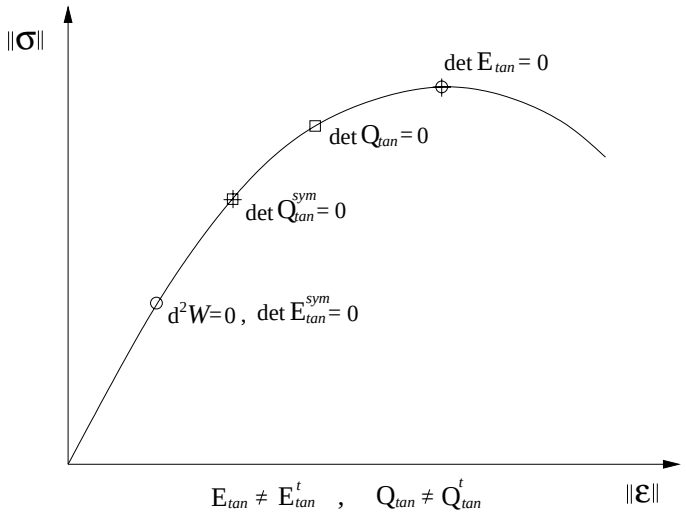

Figure 1: Hierarchy of Failure Indicators for Non-Symmetric Material Models

2.2 Loss of Ellipticity

The loss of ellipticity argument leads to the counterintuitive observation that localization may take place prior to loss of uniqueness. Proceeding along a similar vane as before, we note that the localization tensor $\boldsymbol{Q}_{tan}$ and its singularity [**?**] are affected by the symmetrizing effect of the quadratic form,

$$\boldsymbol{Q}_{tan} = \boldsymbol{N} \cdot \boldsymbol{\mathcal{E}}_{tan} \cdot \boldsymbol{N} \tag{8}$$

Here $\boldsymbol{N}$ denotes the normal vector to the singularity surface along which a weak dicontinuity forms when the localization tensor turns singular, $\det \boldsymbol{Q}_{tan} = 0$. We speak of loss of strong ellipticity when the symmetrized localization tensor turns singular. According to the Bromwich bounds, the loss of strong ellipticity always precedes the loss of ellipticity as

$$\lambda_{min}(\frac{1}{2}[\boldsymbol{Q}_{tan} + \boldsymbol{Q}_{tan}^t]) \leq \Re(\lambda_{min}(\boldsymbol{Q}_{tan})) \tag{9}$$

Beside the hierarchy of strong ellipticity versus ellipticity, the main issue however is, whether and how the loss of ellipticity relates to the loss of material stability and the loss of material uniqueness? Noting that the symmetrizing effect of the single contractions in the quadratic form of the localization indicator eq. 8 are less severe than the double contractions in the quadratic form of the stability indicator eq. 4, the loss of ellipticity is bounded below by the loss of stability and may precede loss of uniqueness in the case of non-symmetric material models.

Figure 1 illustrates the hierarchy of different failure diagnostics, whereby all indicators coincide in the case of symmetric material models taking place at the peak response.

3 THE POLAR CASE

Let us now turn to the issue of second order stress and strain tensors which are non-symmetric.

3.1 Equilibrium of Cosserat Continua [?]

Micropolar continua [?] are characterized by a non-symmetric stress tensor since couple stresses enter the differential statements of equilibrium. Omitting body forces and body couples for the sake of clarity, the local format of linear and angular momenta in the solution domain $\mathcal{D}$ read in direct and index notations:

$$\mathrm{div}(\boldsymbol{\sigma})^t = \mathbf{0} \quad \text{or} \quad \sigma_{ij,i} = 0 \tag{10}$$

and

$$\mathrm{div}(\boldsymbol{\mu})^t + \boldsymbol{e} : \boldsymbol{\sigma} = \mathbf{0} \quad \text{or} \quad \mu_{ij,i} + e_{jkl}\sigma_{kl} = 0 \tag{11}$$

From the second equilibrium equation we note that the stress tensor remains symmetric only if the couple stresses form a self-equilibrating, divergence-free state:

$$\boldsymbol{\sigma} = \boldsymbol{\sigma}^t \quad \Leftrightarrow \quad \boldsymbol{e} : \boldsymbol{\sigma} = \mathbf{0} \qquad \text{if} \qquad \mathrm{div}(\boldsymbol{\mu})^t = \mathbf{0} \tag{12}$$

Here $\boldsymbol{e}$ denotes the third order permutation tensor, while the important details of the lack of symmetry in the indices are shown in figure 2.

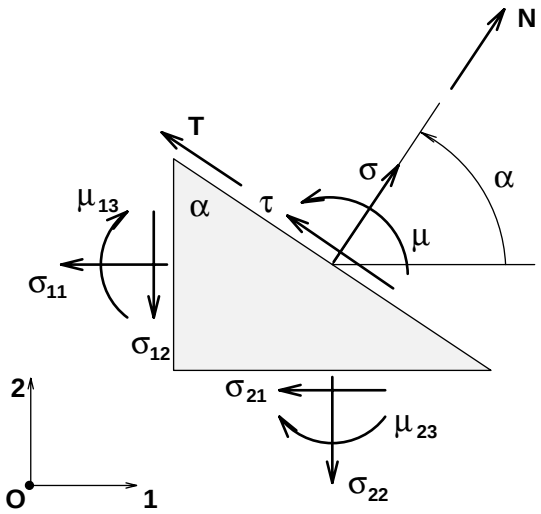

Figure 2: Non-symmetric state stress and couple stress in Cosserat continua

On the stress boundary $\partial\mathcal{D}$ with the normal vector $\boldsymbol{N}$, the complementing conditions of surface tractions and couple stresses read:

$$\boldsymbol{N}\cdot\boldsymbol{\sigma}=\boldsymbol{t}^{\sigma}\quad\text{on }\partial\mathcal{D}^{\sigma}\qquad\text{or}\quad N_i\,\sigma_{ij}=t_j^{\sigma} \tag{13}$$

and

$$\boldsymbol{N}\cdot\boldsymbol{\mu}^t=\boldsymbol{t}^{\mu}\quad\text{on }\partial\mathcal{D}^{\mu}\qquad\text{or}\qquad N_i\,\mu_{i3}=t_3^{\mu} \tag{14}$$

In summary, the non-symmetric stress tensor may be decomposed into symmetric and skew-symmetric components,

$$\boldsymbol{\sigma}=\boldsymbol{\sigma}^{sym}+\boldsymbol{\sigma}^{skew}=\frac{1}{2}[\boldsymbol{\sigma}+\boldsymbol{\sigma}^t]+\frac{1}{2i}[\boldsymbol{\sigma}-\boldsymbol{\sigma}^t] \tag{15}$$

whereby the Bromwich bounds infer,

$$\sigma_{min}=\lambda_{min}(\frac{1}{2}[\boldsymbol{\sigma}+\boldsymbol{\sigma}^t])\le\Re(\lambda_{min}(\boldsymbol{\sigma}))\le\Re(\lambda_{max}(\boldsymbol{\sigma}))\le\lambda_{max}(\frac{1}{2}[\boldsymbol{\sigma}+\boldsymbol{\sigma}^t])=\sigma_{max} \tag{16}$$

and

$$\lambda_{min}(\frac{1}{2i}[\boldsymbol{\sigma}-\boldsymbol{\sigma}^t])\le\Im(\lambda_{min}(\boldsymbol{\sigma}))\le\Im(\lambda_{max}(\boldsymbol{\sigma}))\le\lambda_{max}(\frac{1}{2i}[\boldsymbol{\sigma}-\boldsymbol{\sigma}^t]) \tag{17}$$

This means that the minor and major principal values of symmetrized stress provide lower and upper bounds of the real valued spectrum of the non-symmetric stress tensor. Hereby, the principal directions identify those coordinate axes along which the shear stresses vanish, i.e. when the traction vector is co-axial with the normal vector,

$$\boldsymbol{N}\cdot\boldsymbol{\sigma}=\lambda\boldsymbol{N}\quad\text{such that}\quad\boldsymbol{t}^{\sigma}=\lambda\boldsymbol{N} \tag{18}$$

Therefore, the principal values of the eigenvalue problem coincide with the maximum and minimum normal stress components only in the case of symmetry. In all other cases, the coordinates of maximum and minimum normal stress components are no longer principal coordinates, they exhibit shear stresses which are non-zero when $\boldsymbol{\sigma}\neq\boldsymbol{\sigma}^t$.

On a final note, we consider the three trace invariants in oder to examine the effect of skew-symmetry,

$$\begin{aligned} I_1&=tr\boldsymbol{\sigma}=tr\boldsymbol{\sigma}_{sym}\quad\text{with}\quad tr\boldsymbol{\sigma}_{skew}=0\\ I_2&=\frac{1}{2}tr\boldsymbol{\sigma}^2=\frac{1}{2}\boldsymbol{\sigma}:\boldsymbol{\sigma}=\frac{1}{2}[\boldsymbol{\sigma}_{sym}:\boldsymbol{\sigma}_{sym}+\boldsymbol{\sigma}_{skew}:\boldsymbol{\sigma}_{skew}]\\ I_3&=\frac{1}{3}tr\boldsymbol{\sigma}^3=\frac{1}{3}tr\boldsymbol{\sigma}_{sym}^3+tr(\boldsymbol{\sigma}_{sym}\cdot\boldsymbol{\sigma}_{skew}^2)\end{aligned} \tag{19}$$

We note that the contribution of the skewed stress component vanishes only in the linear trace invariant, while the quadratic and cubic trace invariants exhibit contributions of the skewed-symmetric components.

3.2 Kinematics of Cosserat Continua [?]

The deformation of micropolar continua is characterized by rotational degrees of freedom $\boldsymbol{\omega}:\mathcal{D}\to\mathbb{R}^3$ of the hidden triad in addition to the translatory motion described by the displacement field $\boldsymbol{u}:\mathcal{D}\to\mathbb{R}^3$. Thus, the macro-rotations do no longer coincide with the micro-rotations at each material particle. The infinitesimal

strain tensor features the traditional contribution of the displacement gradients and that of the micro-rotations:

$$\boldsymbol{\epsilon} = \nabla_x^t\, \boldsymbol{u} - \boldsymbol{e}\cdot\boldsymbol{\omega} \qquad \text{or} \qquad \epsilon_{ij} = u_{j,i} - e_{ijk}\omega_k \tag{20}$$

In addition to the non-symmetric strain, the micro-curvature is energetically conjugate to the couple stresses:

$$\boldsymbol{\kappa} = \nabla_x^t\, \boldsymbol{\omega} \qquad \text{or} \qquad \kappa_{ij} = \omega_{j,i} \tag{21}$$

In analogy to the non-symmetric stress tensor, the strain may be decomposed into symmetric and skew-symmetric components, $\boldsymbol{\epsilon} = \boldsymbol{\epsilon}^{sym} + \boldsymbol{\epsilon}^{skew}$, where

$$\boldsymbol{\epsilon}^{sym} = \frac{1}{2}\left[\nabla_x^t\, \boldsymbol{u} + \nabla_x\, \boldsymbol{u}\right] \quad \text{and} \quad \boldsymbol{\epsilon}^{skew} = \frac{1}{2}\left[\nabla_x^t\, \boldsymbol{u} - \nabla_x\, \boldsymbol{u}\right] - \boldsymbol{e}\cdot\boldsymbol{\omega} \tag{22}$$

The symmetric components of the displacement gradient define the infinitesimal strain tensor of the classical continuum, while the skew-symmetric strain components designate the difference between the macro- and micro-rotation. If both rotations coincide, the kinematic relations of classical non-polar continua are retrieved. In view of the decomposition into symmetric and skewed-symmetric components, the non-symmetric strain tensor exhibits the same properties as the non-symmetric stress tensor discussed in the previous section.

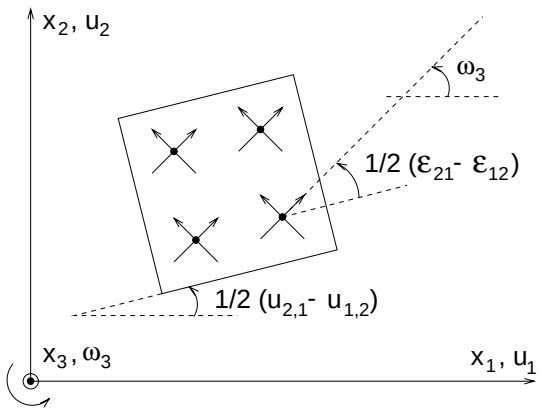

Figure 3: The effect of micro- and macro-rotations in Cosserat continua

Figure 3 illustrates the basic difference between micro-rotations and macro-rotations which is the cause for the lack of symmetry in the strain measure.

4 MOHR'S CIRCLE OF NON-SYMMETRIC STRESS

In what follows, we consider the state of plane stress to illustrate the subtle features of non-symmetric stress with the aid of Mohr's circle [**?**]. The transformation relations for non-symmetric stress in the Mohr plane leads to a circle whose center is no longer located on the σ_N-axis. Defining the normal stress component $\sigma_N = \boldsymbol{N}\cdot\boldsymbol{\sigma}\cdot\boldsymbol{N}$, and the shear stress components $\tau_N = \boldsymbol{N}\cdot\boldsymbol{\sigma}\cdot\boldsymbol{T}$ for an arbitrary surface element with the normal $\boldsymbol{N}$ and the tangent vector $\boldsymbol{T} \perp \boldsymbol{N}$, the extended Cauchy argument in Figure 2 leads to the following transformation relations of stress and couple stress:

$$\left\{ \begin{array}{rcl} \sigma_N &=& \sigma_{11}\ \cos^2\alpha \ + \ \sigma_{22}\ \sin^2\alpha \ + \ (\sigma_{12}+\sigma_{21})\ \sin\alpha\ \cos\alpha \\ \tau_N &=& \sigma_{12}\ \cos^2\alpha \ - \ \sigma_{21}\ \sin^2\alpha \ + \ (\sigma_{22}-\sigma_{11})\ \sin\alpha\ \cos\alpha \end{array} \right. \tag{23}$$

$$\mu = \mu_{13}\ \cos\alpha + \mu_{23}\ \sin\alpha \tag{24}$$

The geometrical representation of the non-symmetric stress transformation results in the generalization of the traditional Mohr circle construction [?], [?]:

$$\boxed{(\sigma_N - \sigma_c)^2 + (\tau_N - \tau_c)^2 = R^2} \tag{25}$$

$$\sigma_c = \frac{\sigma_{11}+\sigma_{22}}{2},\ \ \tau_c = \frac{\sigma_{12}-\sigma_{21}}{2}\ \text{ and }\ R^2 = \left(\frac{\sigma_{11}-\sigma_{22}}{2}\right)^2 + \left(\frac{\sigma_{12}+\sigma_{21}}{2}\right)^2$$

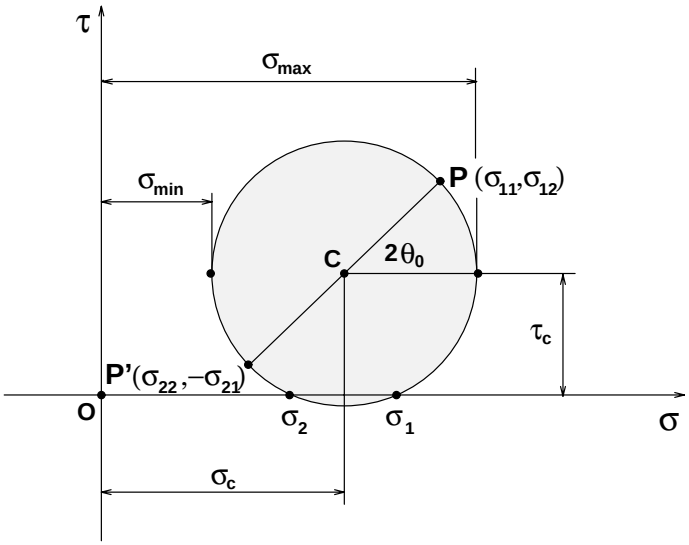

Figure 4: Mohr circle of non-symmetric state of plane stress

Note, the center of Mohr's circle is no longer located on the σ_N-coordinate axis. Clearly, the shift of the center along the shear ordinate is a measure of the loss of symmetry. Figure 4 illustrates the lack of symmetry in the Mohr coordinates of normal and shear stress. Note, that the eigenvalues,

$$\lambda_{1,2} = \sigma_c \pm \sqrt{\frac{1}{4}(\sigma_{11}-\sigma_{22})^2 + \sigma_{12}\sigma_{21}} \tag{26}$$

are the principal stresses $\sigma_{1,2}$ with zero shear. They remain real-valued only as long as the discriminant is positive, i.e.

$$\Delta_\sigma > 0 \quad \text{ as long as } \quad (\sigma_{11}-\sigma_{22})^2 > -\,4\sigma_{12}\ \sigma_{21} \tag{27}$$

Clearly, for conjugate shear stresses this condition is always satisfied. However, when one of the shear components has the opposite sign of the other, then the discriminant might turn negative. The difference in the shear terms between the Mohr circle and the eigenvalue expressions is responsible for the upper and lower bound properties $\sigma_{max} \geq \sigma_1$ and $\sigma_{min} \leq \sigma_2$. When $\Delta_\sigma < 0$, then the two eigenvalues turn complex conjugate. This corresponds to a Mohr circle which no longer intersects the σ_N-axis. In this context it is important to recall the Bromwich bounds according to which

the lowest and highest eigenvalues of the symmetrized stress state enclose the lowest and highest eigenvalues of the non-symmetric state of stress:

$$\sigma_2^{sym} = \sigma_{min} \leq \Re(\boldsymbol{\sigma}) \leq \sigma_{max} = \sigma_1^{sym} \tag{28}$$

4.1 Pure Shear Example

For illustration we consider first the classical example of pure shear [**?**] where the conjugate shear stresses are symmetric, and chosen such to satisfy the traditional J_2-condition of plastic yielding. In this case the Mohr circle is centered at the origin of the $\bar{\sigma} - \bar{\tau}$-coordinate system which has been normalized by the J_2-invariant.

$$\boldsymbol{\sigma} = \begin{bmatrix} 0.0 & 1.1547 \\ 1.1547 & 0.0 \end{bmatrix} \tag{29}$$

In this symmetric case of stress the maximum and minimum values of normal stress components coincide with the principal values and the directions shown in figure 5. In this case, $\sigma_{max} = \sigma_1 = \sigma_{12}$ and $\sigma_{min} = \sigma_2 = -\sigma_{12}$.

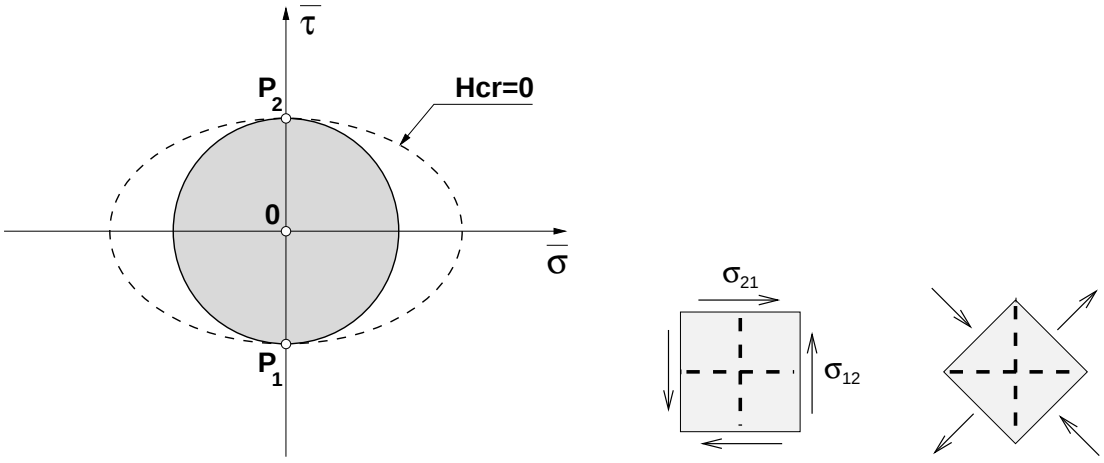

Figure 5: Mohr Circle and Localization Properties in Pure Shear

This figure also includes the localization properties of an elastic perfectly plastic J_2-material for which the critical hardening modulus is zero, $H_{cr} = 0$, at the onset of discontinuous bifurcation. There are two slip planes which develop at $\theta_{cr} = \pm 45^o$ with respect to the direction of maximum normal stress, which corresponds to the contact points P_1 and P_2 of the Mohr circle with the elliptic localization envelope [**?**], [**?**] [**?**]. In summary, this well-known result of classical J_2-plasticity exhibits two slip planes oriented in the horizontal and vertical directions.

4.2 Non-Symmetric Shear Example

As a second example we consider a non-symmetric shear case when $\sigma_{12} = 0$ and $\sigma_{21} = 2.3094$.

$$\boldsymbol{\sigma} = \begin{bmatrix} 0.0 & 0.0 \\ 2.3094 & 0.0 \end{bmatrix} \tag{30}$$

This situation corresponds to the mixed boundary conditions which are often encountered in testing shear walls. The non-symmetric state of stress plots as the

Mohr circle shown in figure 6. Its center is located on the negative τ-axis such that the principal stresses vanish, $\sigma_1 = \sigma_2 = 0$, while the maximum and minimum normal stress coordinates $\sigma_{max} = -\sigma_{min} = \sigma_{21}/2$ involve also the shear stress component $\tau_m = -\sigma_{21}/2$.

The underlying Cosserat formulation of the extended J_2-condition of plastic yielding which includes the effect of the skew-symmetric components in the quadratic invariant of deviatoric stress leads to localization [**?**], when the critical hardening modulus reduces to the softening value $H_{cr} = -E/4$ (using $G_c = G$ for the micropolar shear stiffness). The normal vector of the single slip direction is oriented at $\theta_{cr} = 45^o$ with regard to the maximum normal stress direction. Figure 6 shows that the elliptic localization envelope contacts the Mohr circle of the non-symmetric shear state at the points $P_1 = P_2$. They coincide in this case which indicates loss of ellipticity and formation of a single horizontal slip plane rather than two.

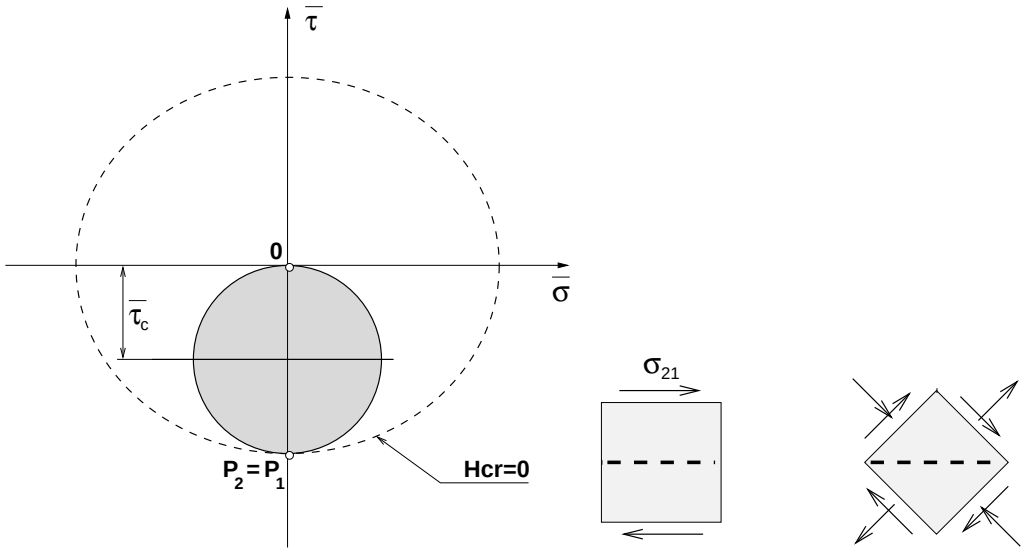

Figure 6: Mohr Circle and Localization Properties in Non-Symmetric Shear

5 CONCLUSIONS

The discussion of the lack of symmetry in mechanics of materials showed a number of perplexing features which can however be explained well by the common aspects of the Bromwich bounds. One of the fascinating concepts is the fundamental role of Mohr's circle which extends to non-symmetric second order tensors. For illustration purposes, our attention was confined to two-dimensional reductions, with the understanding, that generalization of the two-dimensional Mohr circle concept to three-dimensions is by no-means trivial.

6 ACKNOWLEDGEMENTS

The author wishes to thank the Alexander von Humboldt Foundation, Bonn-Bad Godesberg, under grant USA 1056717 for the support in the form of a Research Award.

The article was also partially supported by the National Science Foundation grant CMS 9622940 on *Ultrasonic Assessment of Damage in Concrete Materials* to the University of Colorado Boulder. Opinions expressed in this paper are those of the

writer and do not reflect those of the sponsor.

REFERENCES

[1] Bromwich, T.J. *Quadratic forms and their classification by means of invariant-factors.* Cambridge Tracts in Mathematics and Mathematical Physics, London, (1906).

[2] E. Cosserat and F. Cosserat. *Théorie des corps déformables.* Herman et fils, Paris, (1909).

[3] Eringen, C.A. *Linear theory of micropolar elasticity.* J. of Math. and Mech., **15**, 909-923, (1966).

[4] Iordache, M.-M. and Willam, K. *Localized failure analysis in elastoplastic Cosserat continua*, Comp. Meth. Appl. Mech. Engrg., **151**, 559-586, (1998).

[5] Iordache, M.-M., and Willam, K. *Localization properties of non-symmetric elastoplastic Cosserat formulations*, IV World Congress for Computational Mechanics, June 29-July 2, 1998, Buenos Aires, S. Idlesohn, E. Onate and E.N. Dvorkin (eds.), CD-ROM, Section 7, Paper 8, (1998).

[6] Kuhl, E., Ramm, E. and Willam, K. *Failure Analysis of Elasto-Plastic Materials at Different Levels of Observation*, Intl. J. Solids Structures, **37**, 7259-7280, (2000).

[7] Mohr, O. *Über die Darstellung des Spannungszustandes und des Deformationszustandes eines Körperelementes und über die Anwendung derselben in der Festigkeitslehre.* Civilingenieur, **28**, 113-156, (1882).

[8] Willam, K., Dietsche, A., Iordache, M.-M. and Steinmann, P. *Localization in micropolar continua*, Chapter 9, Continuum Models for Materials with Microstructure, H.-B. Mühlhaus (ed.), John Wiley & Sons, 297-340, (1995).

[9] Willam, K., *Constitutive Models for Materials*, Encyclopedia of Physical Science & Technology, 3rd Edition, Academic Press, (2000). http://civil.colorado.edu/ willam/matls.pdf